Mutation of a Highly Conserved Arginine in Motif IV of *Escherichia coli* DNA Helicase II Results in an ATP-binding Defect*

(Received for publication, March 26, 1997)

Mark C. Hall‡ and Steven W. Matson‡§¶

From the ‡Department of Biology and the §Curriculum in Genetics and Molecular Biology, University of North Carolina, Chapel Hill, North Carolina 27599

A site-directed mutation in motif IV of *Escherichia coli* DNA helicase II (UvrD) was generated to examine the functional significance of this region. The highly conserved arginine at position 284 was replaced with alanine to construct UvrD-R284A. The ability of the mutant allele to function in methyl-directed mismatch repair and UvrABC-mediated nucleotide excision repair was examined by genetic complementation assays. The R284A substitution abolished function in both DNA repair pathways. To identify the biochemical defects responsible for the loss of biological function, UvrD-R284A was purified to apparent homogeneity, and its biochemical properties were compared with wild-type UvrD. UvrD-R284A failed to unwind a 92-base pair duplex region and was severely compromised in unwinding a 20-base pair duplex region. The K_m of UvrD-R284A for ATP was significantly greater than 3 mM compared with 80 μM for UvrD. A large decrease in ATP binding was confirmed using a nitrocellulose filter binding assay. These data suggested that the R284A mutation severely reduced the affinity of helicase II for ATP. The reduced unwinding activity and loss of biological function of UvrD-R284A was probably the result of decreased affinity for ATP. These results implicate motif IV of superfamily I helicases in nucleotide binding and represent the first characterization of a helicase mutation outside motifs I and II that severely impacted the K_m for ATP.

Helicase-catalyzed unwinding of double-stranded nucleic acid molecules is required in all aspects of DNA and RNA metabolism including replication, DNA repair, recombination, transcription, translation, RNA processing, and bacterial conjugation (1–10). Helicases couple the energy derived from hydrolysis of nucleoside 5′-triphosphates (NTPs)[1] to the disruption of hydrogen bonds between the complementary bases of a double helix. The mechanism of unwinding is not known although models have been proposed and are currently being tested (7, 11, 12). These models are based on the formation of active oligomers, which provide multiple DNA binding sites for the helicase. Most, if not all, helicases appear capable of forming either a dimer or hexamer, and evidence suggests that the oligomer is an active species (7).

Helicases are ubiquitous in nature, with numerous examples in viral, prokaryotic, and eukaryotic organisms. Extensive computer-assisted sequence analysis of numerous helicases has uncovered a series of short, conserved amino acid motifs (13–15). This has allowed grouping of helicases into four families based on the extent of amino acid similarity and on the organization of these conserved regions. These families presumably represent evolutionary relationships. Superfamilies I and II are the largest and most closely related groups, whereas superfamily III and family IV have unique motif compositions that differ considerably from those in superfamilies I and II and from each other (16).

Analysis of helicases with mutations in highly conserved residues in several of the so-called "helicase motifs" has suggested a biochemical role of some of these regions in helicase function. For example, motifs I and II, first described as the Walker A and B sequences in a large family of NTP binding proteins (17), have been directly implicated in NTP binding and/or hydrolysis (18–22). The function of the remaining helicase motifs is less clear. Roles for motif VI in nucleic acid binding and ATP hydrolysis have been proposed for various superfamily II RNA helicases (23–25). Motif V has been implicated in single-stranded DNA (ssDNA) binding (26) and motif III in coordination of ATP and ssDNA binding (27) for superfamily I helicases. The recent crystal structure of PcrA, a superfamily I DNA helicase from *Bacillus stearothermophilus*, suggested that all seven of the conserved helicase motifs are clustered together in the vicinity of the ATP binding site (28). Thus, all of the motifs may be involved in ATP binding and/or hydrolysis, at least for those enzymes with structures similar to PcrA.

Escherichia coli DNA helicase II, the product of the *uvrD* gene, is a well characterized DNA helicase. This enzyme is a required component of the UvrABC-mediated nucleotide excision repair pathway (29, 30) and the methyl-directed mismatch repair pathway (31). Less defined roles in recombination and DNA replication have also been suggested (18, 19, 32–40). The purified enzyme unwinds DNA with 3′ to 5′ polarity (41) and is capable of initiating unwinding from a nick, its presumed biological substrate in the repair pathways (42–44). UvrD belongs to helicase superfamily I along with other *E. coli* helicases such as Rep, RecB, RecD, TraI, and helicase IV (*helD* gene product) (13, 16), as well as a large number of eukaryotic viral helicases and several yeast helicases.

UvrD has previously been the subject of biochemical and genetic studies involving mutation of highly conserved residues in motifs I, II, and III (18, 19, 27, 44). Currently, very little biochemical information exists on the specific role of motif IV in superfamily I and II helicases although its importance for biological function has been demonstrated in genetic studies (45–47). In this report, the functional significance of motif IV in *E. coli* DNA helicase II was addressed by site-directed mu-

[1] The abbreviations used are: NTP, nucleoside 5′-triphosphate; ssDNA, single-stranded DNA; LB, Luria broth; ATPγS, adenosine 5′-*O*-(thiotriphosphate); bp, base pair.

tagenesis of arginine residue 284, which is invariant among superfamily I helicases. The results indicated that the mutant protein had a significant decrease in affinity for ATP, implicating motif IV in nucleotide binding. This represents the first helicase mutation outside of motifs I and II that exhibits a severe defect in nucleotide binding.

EXPERIMENTAL PROCEDURES
Materials

Bacterial Strains—*E. coli* BL21(DE3) (F⁻ *ompT* [lon] *hsdS*$_B$ r$_B$⁻ m$_B$⁻ *gal dcm* λDE3) was from Novagen, Inc. *E. coli* JH137 (K91 *lacZ dinD1*::MudI (Ap^r lac)) was obtained from Dr. P. Model (Rockefeller University). BL21(DE3)Δ*uvrD* and JH137Δ*uvrD* were constructed previously in this laboratory (18).

DNA and Nucleotides—pET81F1+ was from Dr. P. J. Laipis (University of Florida), and pET9d, pET11d, and pLysS were from Novagen, Inc. M13mp7 ssDNA was prepared as described previously (48). Unlabeled nucleotides were from U. S. Biochemicals Corp. Radioactively labeled nucleotides were from Amersham Corp. pET9d-UvrD and pET11d-UvrD were constructed previously in this laboratory (18).

Enzymes—Restriction endonucleases, DNA polymerase I (large fragment), phage T4 DNA ligase, phage T7 DNA polymerase, and phage T7 polynucleotide kinase were from New England Biolabs Inc. and used as recommended by the supplier.

To overexpress helicase II prior to purification, a 10-liter culture of mid-log phase BL21(DE3)/pLysS cells containing pET11d-UvrD or a 2-liter culture of mid-log phase BL21(DE3)Δ*uvrD*/pLysS cells containing pET9d-UvrD-R284A were induced for protein expression by adding isopropyl β-D-thiogalactopyranoside to 0.5 mM. Growth was continued for 4 h at 37 °C. Wild-type and mutant helicase II proteins were purified using a procedure described previously (49). The concentration of purified protein was determined by spectrophotometric absorbance readings at 280 nm using the previously published helicase II extinction coefficient of 1.29 ml mg⁻¹ cm⁻¹ (49). Storage buffer for helicase II was 20 mM Tris-HCl (pH 8.3), 200 mM NaCl, 25 mM 2-mercaptoethanol, 1 mM EDTA, 0.5 mM EGTA, and 50% glycerol.

Methods

Site-directed Mutagenesis—The plasmid pET81F1-UvrD (27), containing the full-length helicase II coding sequence cloned behind a T7 promoter, as well as the phage F1 origin of replication, was the template for site-directed mutagenesis by standard procedures (50). The oligonucleotide 5′-GCTGGTAGAGGCGTAGTTTTGCTCC-3′ altered codon 284 of helicase II from CGC(arginine) to GCC(alanine) and disrupted a *Bsr*BI restriction site, allowing the initial screening of mutants by restriction digest. After mutagenesis, a 2.0-kilobase pair *Nco*I-*Bsi*WI DNA fragment containing the desired mutation was sub-cloned into pET9d-UvrD, replacing the wild-type *Nco*I-*Bsi*WI fragment in this plasmid and generating pET9d-UvrD-R284A. The presence of a single mutation at the correct location was verified by sequence analysis of the entire helicase II gene in pET9d-UvrD-R284A using an Applied Biosystems 373A DNA Sequencer.

Genetic Assays—UV irradiation survival was determined as described (19). The frequency of spontaneous mutant formation was determined as follows. Eleven independent transformants of each of the appropriate cell strains were grown overnight under antibiotic selection at 37 °C. Serial dilutions of each of the saturated cultures were made in M9 minimal media salts. Appropriate dilutions were plated on LB agar to determine cell titer and on LB agar plus 100 μg/ml rifampicin to determine the number of spontaneously arising rifampicin-resistant cells. After incubation at 37 °C for at least 24 h, colonies were counted, and the spontaneous mutant frequency was calculated for each strain by dividing the median value of rifampicin-resistant cells by the average total viable cells.

Proteolytic Digestion—Limited chymotrypsin cleavage of UvrD and UvrD-R284A was performed as described previously (51). α-Chymotrypsin (5 ng) was added to reactions (15 μl) containing either 2 μM UvrD (monomer) or 1.8 μM UvrD-R284A (monomer), and the reaction was incubated for 2 min at room temperature (25 °C). Where indicated, 2 μM M13mp7 ssDNA was included. Reactions were stopped with 15 μl of gel loading buffer (250 mM Tris-HCl (pH 6.8), 3.4% SDS, 1.1 M 2-mercaptoethanol, 20% glycerol, 0.01% bromphenol blue) and boiled for 2 min. Products were resolved on a 12% polyacrylamide gel (32:1 cross-linking ratio) in the presence of 0.1% SDS and visualized by staining with Coomassie Brilliant Blue R-250 (Sigma).

Nitrocellulose Filter Binding Assays—The binding of UvrD and

UvrD-R284A to ssDNA was determined by measuring the retention of [³²P]DNA on nitrocellulose filters as described previously (52). Reactions (20 μl) contained 25 mM Tris-HCl (pH 7.5), 3 mM MgCl₂, 20 mM NaCl, 5 mM 2-mercaptoethanol, 50 μg/ml bovine serum albumin, and a [³²P]-labeled 92-bp partial duplex helicase substrate (approximately 1.3 μM nucleotide phosphate) (1.86 × 10⁸ cpm μmol⁻¹). Binding reactions were initiated with UvrD or UvrD-R284A over a concentration range of 0.7–84 nM (monomer). After incubation at 37 °C for 10 min, 1 ml of reaction buffer (pre-warmed at 37 °C) was mixed with each sample, and the entire volume was passed through a nitrocellulose filter at a flow rate of 4 ml/min. Filters were washed twice with 1 ml of pre-warmed reaction buffer, dried, and subjected to liquid scintillation counting. Background binding in the absence of enzyme represented less than 0.5% of the total signal and was subtracted from the experimental data. Apparent K_d values were calculated as described previously (27, 53).

Binding of [³H]ATP to UvrD was also examined by nitrocellulose filter binding. Reactions (20 μl) contained 25 mM Tris-HCl (pH 7.5), 3 mM MgCl₂, 50 mM NaCl, 6.3 mM 2-mercaptoethanol, 100 μg/ml bovine serum albumin, 12.5% glycerol, and 2.3 μM UvrD or UvrD-R284A (monomer). Binding was initiated by addition of [³H]ATP (1.1 Ci/mmol) to a final concentration of 200 μM at 0 °C. After 4 min, 15 μl of each reaction was applied directly to a nitrocellulose filter presoaked in reaction buffer at 4 °C. Filters were rinsed once with 750 μl of reaction buffer at a flow rate of 4 ml/min, dried, and subjected to liquid scintillation counting. Background binding in the absence of enzyme represented less than 1% of the total signal and was subtracted from the experimental data. The nitrocellulose filters used in the DNA and ATP binding experiments (0.45 μM type HA, Millipore Corp.) were pre-treated by soaking in 0.4 M KOH for 40 min followed by extensive washing with deionized, distilled water.

Glutaraldehyde Cross-linking—The presence of a dimeric helicase II species was monitored by glutaraldehyde cross-linking as described previously (27, 49). Reactions (20 μl) contained 20 mM Tricine (pH 8.3), 50 mM NaCl, 5 mM MgCl₂, 5 mM 2-mercaptoethanol, 18% glycerol, and either 1.5 μM UvrD (monomer) or 1.4 μM UvrD-R284A (monomer). When present, the oligonucleotide (dT)₁₀ and ATPγS were included at a concentration of 1.7 μM and 3 mM, respectively. Cross-linking was initiated by the addition of glutaraldehyde (EM grade, Electron Microscopy Sciences) to a final concentration of 0.01%. Reactions were incubated at room temperature for 30 min and then quenched with 2 μl of 100 mM lysine acetate and 20 μl of gel-loading buffer (see above). Samples were boiled for 2 min, and the products were resolved on a 9.6% polyacrylamide gel (32:1 cross-linking ratio) in the presence of 0.1% SDS.

Helicase Assays—The DNA unwinding activity of UvrD and UvrD-R284A was determined with 92- and 20-bp partial duplex [³²P]DNA substrates prepared as described previously (19, 41). Both substrates were purified by gel filtration on a Bio-Gel A5M column (Bio-Rad) prior to use. Helicase reactions (20 μl) contained 25 mM Tris-HCl (pH 7.5), 3 mM MgCl₂, 20 mM NaCl, 5 mM 2-mercaptoethanol, 3 mM ATP, and the indicated partial duplex DNA substrate (approximately 1.3 μM nucleotide phosphate) (1.8 × 10⁸ cpm μmol⁻¹ for the 92-bp substrate and 1.6 × 10⁸ cpm μmol⁻¹ for the 20-bp substrate). Reactions were pre-warmed at 37 °C and initiated with the indicated amount of UvrD or UvrD-R284A. After incubation at 37 °C for 10 min, the reactions were quenched with 10 μl of stop solution (37.5% glycerol, 50 mM EDTA, 0.05% each of xylene cyanol and bromphenol blue, and 0.3% SDS). Products were resolved on an 8% non-denaturing polyacrylamide gel, and the results were quantified using phosphor storage technology and ImageQuant software (Molecular Dynamics).

ATPase Assays—The DNA-stimulated hydrolysis of ATP by UvrD and UvrD-R284A was measured as described previously (54). ATPase reaction mixtures were identical to those for the helicase reactions with the following exceptions. M13mp7 ssDNA (30 μM nucleotide phosphate) was substituted for the partial duplex helicase substrate, and [³H]ATP was substituted for unlabeled ATP. Reactions (20 μl) were pre-warmed at 37 °C and initiated with the indicated amount of [³H]ATP. Reactions were incubated at 37 °C, and duplicate samples (5 μl) were removed and quenched with 5 μl of stop solution (33 mM EDTA, 7 mM ATP, and 7 mM ADP) after 5 min for UvrD or 10 min for UvrD-R284A. Products were processed as described previously (54).

RESULTS

DNA helicase II (also called UvrD) has been included, along with a large number of other helicases and putative helicases, in a group designated helicase superfamily I based on conservation of amino acid sequence in seven distinct motifs (13, 15).
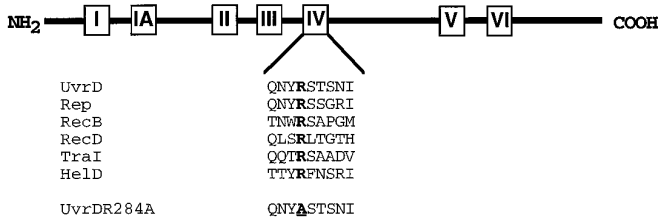
FIG. 1. **The motif structure of superfamily I helicases and the location of the UvrD-R284A mutation.** The approximate positions of the seven conserved motifs of superfamily I helicases are shown in UvrD. The amino acid sequences of motif IV of the *E. coli* members of this helicase family are also shown along with the sequence of UvrD-R284A. The alignments of UvrD, Rep, RecB, and RecD are from Hodgman (15). TraI and HelD sequences were added to this alignment.

TABLE I
Spontaneous mutant frequencies of JH137 and JH137 derivatives

The spontaneous mutant frequency was determined as described under "Experimental Procedures." Relative mutability was obtained by dividing the mutant frequency of each strain by the mutant frequency of JH137.

Strain	Relevant genotype	Spontaneous mutant frequency	Relative mutability
		$\times 10^{-9}$	
JH137	$uvrD^+$	3.0	1
JH137$\Delta uvrD$	$\Delta uvrD$	485	161
JH137$\Delta uvrD$/pET9d-UvrD	$uvrD^+$	1.8	0.6
JH137$\Delta uvrD$/pET9d-UvrD-R284A	$uvrD$-R284A	362	121

Presumably, these motifs represent sites of functional significance that have been evolutionarily conserved. The amino acid sequences of motif IV from the *E. coli* superfamily I helicases, including UvrD, are shown in Fig. 1. To evaluate the functional significance of motif IV, a mutant *uvrD* allele was constructed containing an arginine to alanine substitution at position 284 (*uvrD-R284A*). This arginine is the most highly conserved residue in motif IV. It is found in all identified members of superfamily I. The ability of the mutant protein to substitute for the wild-type protein in two DNA repair pathways was examined in genetic complementation studies. In addition, the UvrD-R284A protein was purified and biochemically characterized.

Genetic Characterization of UvrD-R284A

DNA helicase II is an essential component of two DNA repair pathways, methyl-directed mismatch repair and UvrABC-mediated nucleotide excision repair (29–31). The ability of UvrD-R284A to function in each pathway was tested using genetic complementation assays. The frequency of spontaneous mutant formation in *E. coli* strain JH137$\Delta uvrD$ was 161-fold higher than its parent strain JH137 due to loss of a functional methyl-directed mismatch repair system (55, 56). JH137$\Delta uvrD$ was also highly sensitive to UV light due to loss of UvrABC-mediated nucleotide excision repair (57). Plasmids pET9d-UvrD and pET9d-UvrD-R284A were transformed into JH137$\Delta uvrD$ to examine the ability of UvrD and UvrD-R284A to restore the wild-type spontaneous mutant frequency and UV resistance. The level of uninduced expression of the *uvrD* gene from pET9d-UvrD in JH137$\Delta uvrD$ was determined previously and was only slightly less than expression from the JH137 chromosome (18). This was confirmed in this study (data not shown).

The frequency of formation of spontaneous mutants at the *rpoB* locus (Rif^r phenotype) was determined as described under "Experimental Procedures." Wild-type *uvrD*, when introduced on the pET9d plasmid, fully restored methyl-directed mismatch repair function as indicated by a relative mutability of 0.6 compared with 1.0 for the parental strain JH137 (Table I).
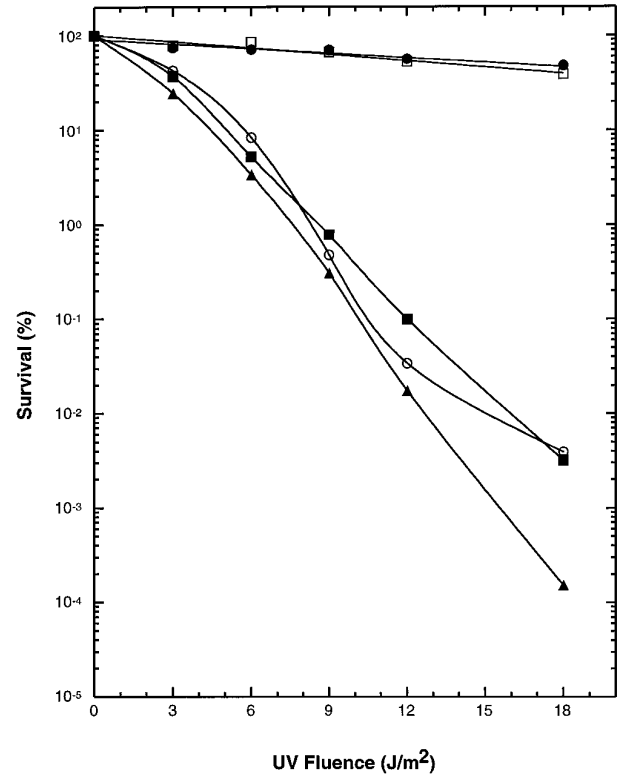

FIG. 2. **UV light survival of JH137 and derivatives.** *E. coli* strains JH137 (●), JH137$\Delta uvrD$ (○), JH137$\Delta uvrD$/pET9d (■), JH137$\Delta uvrD$/pET9d-UvrD (□), and JH137$\Delta uvrD$/pET9d-UvrD-R284A (▲) were exposed to UV light, and survival was calculated as described under "Experimental Procedures." The data represent the average of three independent trials for each strain.

In contrast, the presence of the *uvrD-R284A* allele in JH137$\Delta uvrD$ resulted in a relative mutability of 121, suggesting that the mutant protein did not function in the methyl-directed mismatch repair pathway.

The ability of UvrD-R284A to function in UvrABC-mediated nucleotide excision repair was assessed by exposing cells to UV light and determining survival at increasing UV fluences. Strains JH137, JH137$\Delta uvrD$, JH137$\Delta uvrD$/pET9d, JH137$\Delta uvrD$/pET9d-UvrD, and JH137$\Delta uvrD$/pET9d-UvrD-R284A were compared as shown in Fig. 2. pET9d-UvrD completely restored the wild-type level of UV resistance. The mutant allele did not restore wild-type UV resistance and appeared to make the cells slightly hypersensitive to UV light as compared with JH137$\Delta uvrD$. The significance of the latter observation was not explored. It was clear that UvrD-R284A was not able to substitute for UvrD in UvrABC-mediated nucleotide excision repair.

Biochemical Characterization of UvrD-R284A

To identify the biochemical defects responsible for the loss of biological function of UvrD-R284A, mutant and wild-type helicase II were purified as described previously (49). UvrD was purified to apparent homogeneity as evidenced by the presence of a single protein species on an SDS-polyacrylamide gel (Fig. 3, *lane A*). Purified UvrD-R284A was contaminated by three faint species migrating slightly faster than UvrD-R284A (Fig. 3, *lane D*). These species appeared to be proteolytic products of UvrD-R284A because they all reacted strongly with anti-helicase II antibody (data not shown). This suggested that the mutant enzyme was somewhat less stable than the wild-type enzyme. However, UvrD-R284A folded normally as indicated by a chymotrypsin cleavage pattern that was identical to that of UvrD (Fig. 3, *lanes B* and *E*). In the presence of ssDNA, both UvrD-
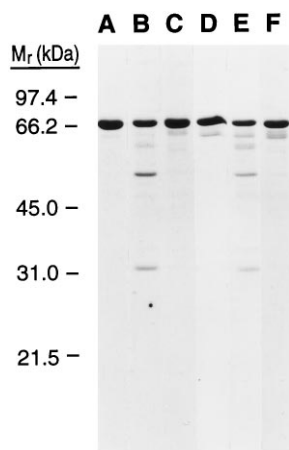
FIG. 3. **α-Chymotrypsin digestion of UvrD and UvrD-R284A.** UvrD and UvrD-R284A were subjected to limited proteolytic digestion by α-chymotrypsin as described under "Experimental Procedures." *Lanes A* and *D*, purified UvrD and UvrD-R284A, respectively; *lanes B* and *E*, the products of the UvrD and UvrD-R284A proteolysis reactions, respectively; *lanes C* and *F*, 2 μM M13mp7 ssDNA was added to the UvrD and UvrD-R284A proteolysis reactions. The UvrD concentration was 2 μM (monomer), and the UvrD-R284A concentration was 1.8 μM (monomer). The molecular mass standards were: rabbit muscle phosphorylase b (97.4 kDa), bovine serum albumin (66.2 kDa), hen egg white ovalbumin (45.0 kDa), bovine carbonic anhydrase (31.0 kDa), and soybean trypsin inhibitor (21.5 kDa).

FIG. 4. **DNA binding by UvrD and UvrD-R284A.** Nitrocellulose filter binding assays were used to evaluate DNA binding as described under "Experimental Procedures" using UvrD (●) or UvrD-R284A (■). Data represent the average of at least three independent trials, and *error bars* are the standard deviations.

R284A and UvrD were protected from chymotrypsin cleavage (Fig. 3, *lanes C* and *F*). Furthermore, proteolytic products did not accumulate with long term enzyme storage. Given these results and the minimal representation of the smaller species in the total protein, it was unlikely that their presence influenced the data presented in this study.

DNA Binding—The ability of UvrD-R284A to bind to DNA was tested using a nitrocellulose filter binding assay and the 92-bp partial duplex helicase substrate. Although the substrate contains a short duplex region, the assay measured primarily the affinity of the protein for ssDNA due to the lack of significant binding of helicase II to double-stranded DNA. DNA binding isotherms were generated using a constant ligand concentration and varying concentrations of helicase II (Fig. 4). A Hill plot was used to calculate apparent equilibrium dissociation constants from these data as described previously (27, 53). There was no significant difference between the DNA binding properties of UvrD-R284A and UvrD (apparent K_d of 11 and 17 nM, respectively). Thus, the highly conserved arginine residue in motif IV was not required for nucleic acid binding. This conclusion was further supported by the results of limited proteolysis experiments (see Fig. 3), which demonstrated that both UvrD and UvrD-R284A were protected from chymotrypsin cleavage when an ssDNA ligand was present and presumably bound by the enzyme.

Dimerization—A glutaraldehyde cross-linking procedure was used to detect dimerization of UvrD and UvrD-R284A (49). Glutaraldehyde catalyzes the formation of a covalent bond between primary amines in close proximity, providing a simple method for detecting protein-protein interactions in solution. UvrD and UvrD-R284A, at a relatively high concentration, were each exposed to a low concentration of glutaraldehyde in the absence or presence of ATPγS or oligonucleotide (dT)$_{10}$. The products were resolved on an SDS-polyacrylamide gel and stained with Coomassie Blue. No difference in the dimerization of UvrD and UvrD-R284A was observed in the absence or presence of ATPγS or oligo(dT)$_{10}$ (data not shown).

ATP Hydrolysis—Helicase II catalyzes a DNA-stimulated ATP hydrolysis reaction that is coupled to the unwinding re-
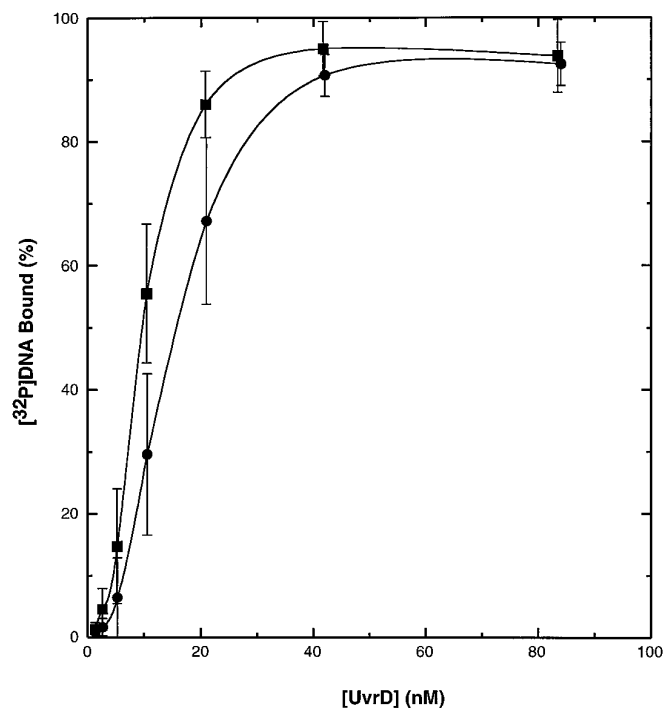
action. To begin to evaluate the ATPase activity of UvrD-R284A, we attempted to measure a K_m for ATP. Wild-type UvrD exhibited a standard hyperbolic saturation curve as a function of increasing ATP concentration with a K_m of 80 ± 7 μM (Fig. 5A). The K_m value of UvrD-R284A for ATP was too high to be determined because the maximal velocity could not be approached. The velocity of ATP hydrolysis catalyzed by UvrD-R284A was a linear function of ATP concentration up to 3 mM (Fig. 5B). Apparent substrate inhibition of the wild-type enzyme prevented accurate measurement of ATP hydrolysis velocities at substantially higher ATP concentrations (data not shown). The inability to saturate UvrD-R284A with ATP suggested that it was defective in nucleotide binding.

ATP Binding—To directly measure the affinity of helicase II for ATP, an initial attempt was made to determine the equilibrium dissociation constant, K_d. Several techniques were used without success, including fluorescence spectroscopy and nitrocellulose filter binding. Failure to determine a K_d was the result of the limited solubility of helicase II and its relatively low affinity for ATP, which made it impossible to generate a complete and reproducible binding curve using these assays. In addition, we did not observe an intrinsic fluorescence change in helicase II upon ATP binding. However, having a K_d for the UvrD-ATP interaction would not be useful for comparative purposes if we were unable to measure this value for UvrD-R284A. Instead, nitrocellulose filter binding assays were used as a qualitative comparison of ATP binding between UvrD and UvrD-R284A by measuring the amount of [³H]ATP bound at a single nucleotide concentration. These assays were performed at 0 °C and in the absence of DNA. Under these conditions, the turnover number for wild-type helicase II was approximately 0.002 s^{-1} (data not shown). Table II shows that at 200 μM [³H]ATP, UvrD bound 0.92 pmol of ATP/pmol of enzyme. This fraction of ATP-bound enzyme was fairly consistent with a K_m of 80 μM ATP. In contrast, UvrD-R284A bound only 0.015 pmol of ATP/pmol of enzyme, 1.6% of the wild-type value. These

FIG. 5. **ATP hydrolysis by UvrD and UvrD-R284A.** ATP hydrolysis was measured as described under "Experimental Procedures" for UvrD (*panel A*) and UvrD-R284A (*panel B*). Reactions containing 2.1 nM UvrD or 229 nM UvrD-R284A (monomer) were initiated with the indicated concentration of [^{3}H]ATP and incubated at 37 °C for 5 min (UvrD) or 10 min (UvrD-R284A). SigmaPlot (Jandel Scientific) was used to fit the data for UvrD in *panel A* to a standard rectangular hyperbola and to generate the linear regression for UvrD-R284A in *panel B*. The *inset* in *panel A* represents an Eadie-Hofstee plot of the data shown in *panel A*. K_m was calculated from the Eadie-Hofstee plot. The data in both *panels A* and *B* are averages obtained from at least three independent experiments with *error bars* representing standard deviations.
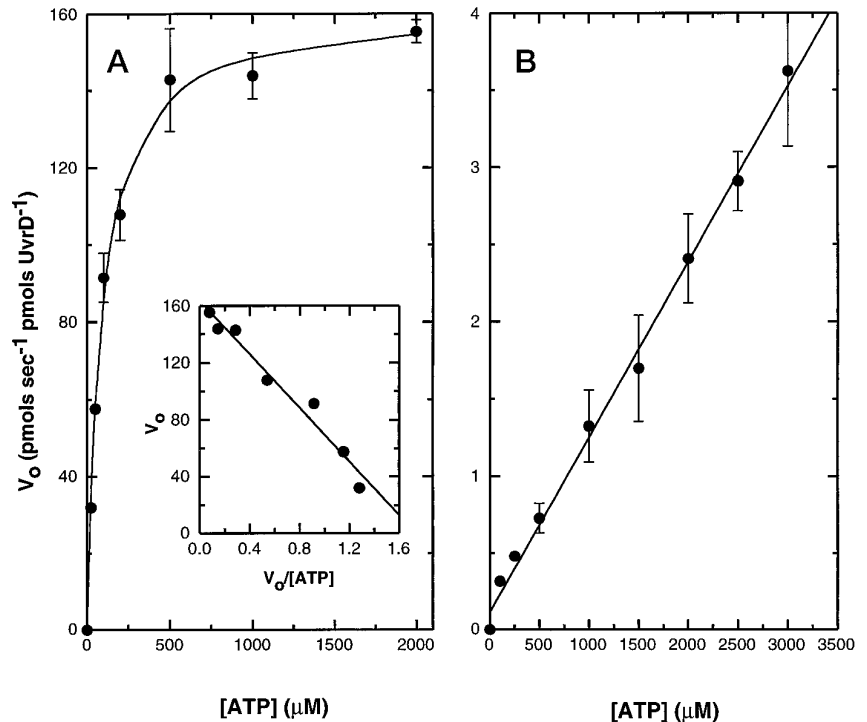
TABLE II
ATP binding by UvrD and UvrD-R284A

ATP binding was measured by a nitrocellulose filter assay as described under "Experimental Procedures." UvrD and UvrD-R284A were 2.3 μM (monomer) and [^{3}H]ATP was 200 μM in the reactions. Data represent the average of eight independent trials.

Enzyme	pmol bound per pmol of enzyme
UvrD	0.92
UvrD-R284A	0.015

results suggested that UvrD-R284A was defective in its association with ATP.

Helicase Activity—The lack of genetic complementation in both DNA repair pathways suggested that the mutant protein was severely compromised in its DNA unwinding activity. The unwinding activity of UvrD-R284A was measured using two short partial duplex DNA substrates and was compared with UvrD (Fig. 6). The mutant enzyme failed to catalyze unwinding of a 92-bp duplex region and catalyzed feeble unwinding of a 20-bp duplex region in a 10-min incubation. At a UvrD-R284A concentration of 344 nM, there was no detectable unwinding of the 92-bp partial duplex substrate and less than 10 percent unwinding of the 20-bp partial duplex substrate. In contrast, wild-type helicase II unwound 50% of the 92-bp partial duplex substrate at a protein concentration of 25 nM and 50% of the 20-bp partial duplex substrate at a protein concentration of 0.5 nM. In a 100-min incubation, 197 nM UvrD-R284A unwound 39% of the 20-bp partial duplex. Under the same conditions, 344 nM mutant enzyme did not unwind a detectable fraction of the 92-bp substrate (data not shown).

DISCUSSION

The results presented here indicate that arginine 284 is required for high affinity binding of ATP, which suggests that motif IV is an integral part of the nucleotide binding site on DNA helicase II. This was initially surprising since it is generally believed that helicase motifs I and II are involved in NTP binding and/or hydrolysis. This notion stems from the fact that motifs I and II are common to a large population of NTP-binding proteins, including the DNA helicases (17). Moreover, biochemical studies on mutants of a wide range of helicases have generally supported a role for motifs I and II in NTP hydrolysis (18–22). Most of the mutations, however, did not affect NTP binding. Helicase motif IV is not conserved among all NTP binding proteins, which suggested that it might be important for a biochemical property common to helicases. However, UvrD-R284A exhibited a significant defect in ATP binding, and in light of the recent crystal structure of PcrA, this result can be readily explained (see below).

Efforts to define the kinetic parameters K_m and k_{cat} for the DNA-stimulated ATP hydrolysis reaction revealed an inability to saturate UvrD-R284A with ATP. Since the ATPase reaction velocity was a linear function of ATP concentration up to 3 mM, the K_m for ATP must be much greater than 3 mM. K_m is defined as the concentration of substrate that provides half-maximal reaction velocity. If it is assumed that the ATPase reaction catalyzed by helicase II can be described by simple Michaelis-Menten kinetics and that a minimal reaction is represented by the following scheme, where S is ATP,

$$E + S \underset{k_{-1}}{\overset{k_1}{\rightleftharpoons}} ES \overset{k_2}{\longrightarrow} E + P$$
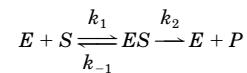
then K_m is equal to $(k_{-1} + k_2)/k_1$. If k_2 is small compared with the dissociation rate constant k_{-1}, then K_m is equal to the equilibrium dissociation constant, K_d (k_{-1}/k_1). However, if k_2 is comparable with k_{-1}, then ES is not in equilibrium with $E + S$, and K_m is not equal to K_d. Furthermore, K_m does not approximate K_d if multiple enzyme-bound intermediates are on the reaction pathway. In the case where multiple intermediates exist, K_m reflects an overall dissociation constant for all of the enzyme-bound species (58). Because the kinetic mechanism for ATP hydrolysis catalyzed by helicase II is not known, it was not possible to unequivocally conclude that the large increase in the K_m value of UvrD-R284A was the direct result of a decreased affinity for ATP. For example, a decrease in the rate of product release or changes in rate constants associated with conformational changes could also affect K_m. In fact, it is possible to envision a kinetic mechanism in which an increase in
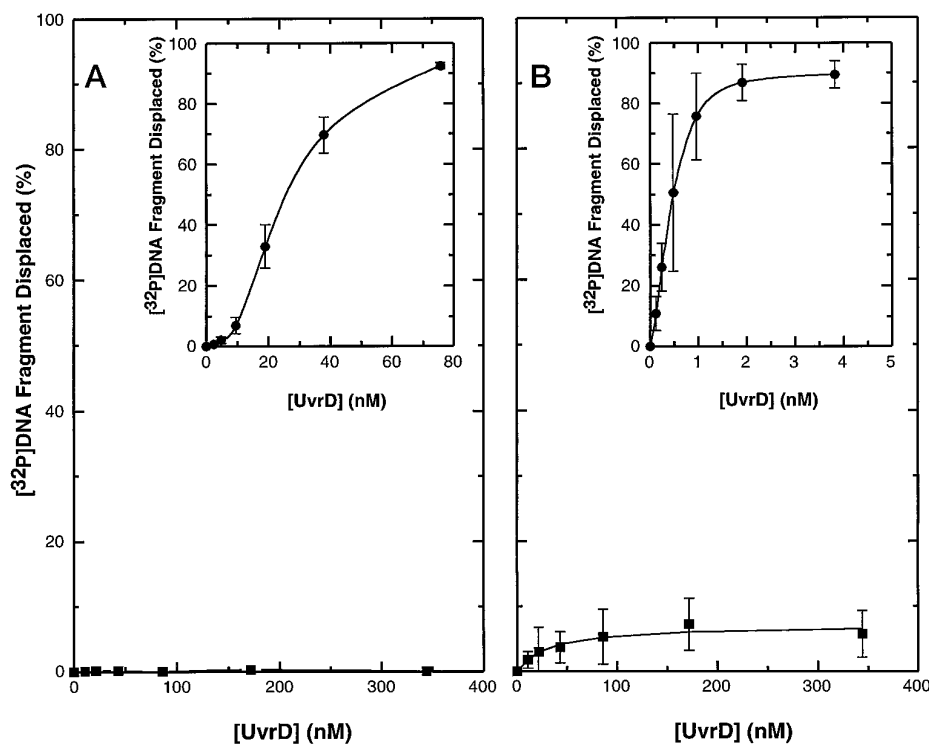
FIG. 6. **Helicase activity of UvrD and UvrD-R284A.** The unwinding of 92-bp (*panel A*) and 20-bp (*panel B*) partial duplex DNA substrates by UvrD (●) and UvrD-R284A (■) was measured as described under "Experimental Procedures." Data represent the average of at least three independent experiments, and *error bars* are standard deviations.

K_m is not related to ATP binding but, rather, is solely the result of a decrease in the rate of hydrolysis. Such a mechanism is very unlikely for helicase II, however, because several UvrD mutants have been characterized that exhibited a significant decrease in the k_{cat} for ATP hydrolysis without affecting K_m (18, 19, 44).

To isolate and evaluate the initial ATP binding event, conditions were sought under which a negligible amount of ATP hydrolysis occurred. At 0 °C in the absence of DNA, the turnover number for ATP by UvrD was approximately 0.002 s^{-1}. No hydrolysis was detected under these conditions using UvrD-R284A. Thus, the nitrocellulose filter binding assay likely measured only $E + S \rightleftarrows ES$, again assuming the simple Michaelis-Menten scheme depicted above. Since the amount of ATP bound by UvrD-R284A was significantly decreased under these conditions, a decreased affinity for ATP was likely the primary defect in the mutant protein. Thus, the large increase in K_m for ATP was the result of a decreased affinity for the substrate.

A defect in ATP binding would seem to be at odds with the results of proteolysis protection experiments (data not shown). The presence of ATP, like ssDNA, protects wild-type helicase II from cleavage by chymotrypsin (51). Based on the decreased binding of ATP by UvrD-R284A, we expected to see a large difference in the amount of ATP required to protect UvrD *versus* UvrD-R284A from proteolytic cleavage. In fact, the increase in the concentration of ATP required for protection of UvrD-R284A compared with UvrD was relatively small (less than 2-fold, data not shown). However, the structural changes responsible for proteolysis protection when ligands are present are not known. This fact, coupled with the lack of information on the kinetic mechanism for ATP hydrolysis catalyzed by helicase II, makes it possible that the proteolysis protection assay does not directly measure ATP binding. For example, an ATP concentration of 1.5–2.0 mM was required for significant protection of UvrD from cleavage by chymotrypsin. This is clearly inconsistent with a K_m for ATP of 80 μM. This fact alone indicates that this assay measures something more complex than simple ATP binding. Furthermore, when the poorly hy-

drolyzed ATP analog ATPγS was used as a ligand, there was a more substantial increase in the concentration required for proteolytic protection of UvrD-R284A compared with UvrD (approximately 6-fold, data not shown). The results of the proteolysis protection study likely reflected a combination of processes such as ATP hydrolysis and conformational changes in the protein, in addition to nucleotide binding. Thus, the results of this series of experiments, while not fully explained, cannot be interpreted as evidence for a normal interaction with ATP.

Although there was clearly a serious defect in nucleotide binding, it was also possible that an additional defect existed in the hydrolytic mechanism. Such a defect would also have contributed to the inability of UvrD-R284A to unwind DNA and function in DNA repair pathways. It was possible to estimate a K_m for UvrD-R284A from the data in Fig. 5 if we assumed the hydrolytic mechanism was unaffected. The initial slope of a reaction velocity *versus* substrate concentration graph, such as the one depicted in Fig. 5, is equal to $k_{cat}/K_m \times E_T$, where E_T is the total enzyme concentration. If the hydrolytic mechanism of UvrD-R284A were unaffected by the mutation, then k_{cat} should have been equal to that of UvrD. From the slope of the line in Fig. 5B and the UvrD k_{cat} of 162 s^{-1}, an estimated K_m for ATP for UvrD-R284A was 143 mM. The plot of initial velocity *versus* substrate concentration for UvrD-R284A was linear to at least 3 mM ATP. Since there was no deviation from linearity, it was concluded that the actual K_m was significantly higher than 3 mM. Apparent substrate inhibition with wild-type helicase II at high ATP concentrations, coupled with the necessary modifications in reaction conditions, made it impossible to accurately measure hydrolysis at ATP concentrations significantly higher than 3 mM. Therefore, the relationship between the apparent K_m for ATP and the 143 mM value estimated above was not determined. In light of these results, it remains possible that there was a defect in the hydrolytic mechanism of UvrD-R284A in addition to the severe defect in ATP binding.

The helicase activity of the UvrD-R284A mutant was significantly compromised, and the protein failed to function *in vivo*. Helicase activity is dependent on ATP hydrolysis, and it seemed reasonable to conclude that the lack of unwinding was

due to the tremendous decrease in ATP hydrolysis that, in turn, was due to a decreased affinity of the mutant enzyme for ATP. However, the possibility that the R284A substitution also directly impaired the unwinding mechanism or the coupling between hydrolysis and unwinding cannot formally be ruled out. Based on the results presented here, the lack of biological function in both DNA repair pathways was probably a result of the ATP binding defect. With a K_m for ATP significantly greater than 3 mM, it is unlikely that an intracellular ATP concentration of 3 mM (59) would be sufficient to adequately populate the active helicase II pool and allow the enzyme to function properly *in vivo*.

To the best of our knowledge, UvrD-R284A represents the first helicase mutant, outside of motifs I and II, whose primary defect is in nucleotide binding. A helicase II mutant in motif III was defective in binding ATP but only in the absence of ssDNA (27). This mutant was also defective in binding ssDNA in the absence of ATP. In the presence of ssDNA, the motif III mutant bound ATP with normal affinity, and it was concluded that the motif III mutant was compromised in the ability to form stable binary complexes with its two ligands.

The ATP binding defect described in this study is consistent with the recently published crystal structure of the PcrA helicase (28). The overall amino acid sequence of the PcrA helicase from *B. stearothermophilus* is 44% identical to UvrD and 90% identical within the seven conserved helicase motifs. Notably, these seven motifs are clustered together at the base of the enzyme, forming the ATP-binding pocket. In view of the extensive amino acid identity, particularly among the conserved motifs, it is likely that the structure of the nucleotide binding sites of PcrA and UvrD closely resemble one another. From this structure, it seems likely that all seven motifs may be involved in nucleotide binding and/or hydrolysis, and thus, a role for motif IV in ATP binding is not surprising.

The PcrA structure indicates that motif IV forms a bridge connecting the two large domains of the protein at the bottom of the nucleotide binding pocket. This region lies near the adenine base of the bound nucleotide, and the authors suggest that a conserved tyrosine in motif IV makes a stacking interaction with the bound NTP. This tyrosine, which is not conserved in all superfamily I helicases, is immediately followed by the invariant arginine that was altered in this study (see Fig. 1). The apparent absence of additional specific interactions between the adenine base and nearby amino acid residues was suggested as an explanation for the lack of nucleotide specificity in reactions catalyzed by the PcrA helicase. UvrD, on the other hand, exhibits a strong preference for ATP or dATP (60), and it is possible that arginine 284 is involved in a specific interaction with the adenine base on ATP and dATP, whereas its counterpart in PcrA contributes less to specificity. Alternatively, arginine 284 may not directly contact the nucleotide but might mediate a local conformational change that places other residues, such as tyrosine 283, in proper position to interact with the NTP. Yet another possibility is that motif IV, acting as a bridge between the two large domains of the helicase, might mediate a global conformational change in the protein that is required for high affinity NTP binding. A more detailed description of the role of arginine 284 in ATP binding must await a high resolution structure for ATP-bound helicase II.

REFERENCES

1. Ray, B. K., Lawson, T. G., Kramer, J. C., Cladaras, M. H., Grifo, J. A., Abramson, R. D., Merrick, W. C., and Thach, R. E. (1985) *J. Biol. Chem.* **260,** 7651–7658
2. Schmid, S. R., and Linder, P. (1992) *Mol. Microbiol.* **6,** 283–292
3. Wasserman, D. A., and Steitz, J. A. (1991) *Nature* **349,** 463–464
4. Brennan, C. A., Dombroski, A. J., and Platt, T. (1987) *Cell* **48,** 945–952
5. Lohman, T. M. (1992) *Mol. Microbiol.* **6,** 5–14
6. Lohman, T. M. (1993) *J. Biol. Chem.* **268,** 2269–2272
7. Lohman, T. M., and Bjornson, K. P. (1996) *Annu. Rev. Biochem.* **65,** 169–214
8. Matson, S. W., and Kaiser-Rogers, K. A. (1990) *Annu. Rev. Biochem.* **59,** 289–329
9. Matson, S. W. (1991) *Prog. Nucleic Acid Res. Mol. Biol.* **40,** 289–326
10. Matson, S. W., George, J. W., and Bean, D. W. (1994) *Bioessays* **16,** 13–22
11. Wong, I., and Lohman, T. M. (1992) *Science* **256,** 350–355
12. Makhov, A. M., Boehmer, P. E., Lehman, I. R., and Griffith, J. D. (1996) *J. Mol. Biol.* **258,** 789–799
13. Gorbalenya, A. E., Koonin, E. V., Donchenko, A. P., and Blinov, V. M. (1988) *FEBS Lett.* **235,** 16–24
14. Gorbalenya, A. E., Koonin, E. V., Donchenko, A. P., and Blinov, V. M. (1989) *Nucleic Acids Res.* **17,** 4713–4729
15. Hodgman, T. C. (1988) *Nature* **333,** 22–23
16. Gorbalenya, A. E., and Koonin, E. V. (1993) *Curr. Opin. Struct. Biol.* **3,** 419–429
17. Walker, J. E., Saraste, M., Runswick, M. J., and Gay, N. J. (1982) *EMBO J.* **1,** 945–951
18. George, J. W., Robert M. Brosh, J., and Matson, S. W. (1994) *J. Mol. Biol.* **235,** 424–435
19. Brosh, R. M., Jr., and Matson, S. W. (1995) *J. Bacteriol.* **177,** 5612–5621
20. Washburn, B. K., and Kushner, S. R. (1993) *J. Bacteriol.* **175,** 341–350
21. Pause, A., and Sonenberg, N. (1992) *EMBO J.* **11,** 2643–2654
22. Zavitz, K. H., and Marians, K. J. (1992) *J. Biol. Chem.* **267,** 6933–6940
23. Fernandez, A., Lain, S., and Garcia, J. A. (1995) *Nucleic Acids Res.* **23,** 1327–1332
24. Gross, C. H., and Shuman, S. (1996) *J. Virol.* **70,** 1706–1713
25. Pause, A., Methot, N., and Sonenberg, N. (1993) *Mol. Cell. Biol.* **13,** 6789–6798
26. Graves-Woodward, K. L., and Weller, S. K. (1996) *J. Biol. Chem.* **271,** 13629–13635
27. Brosh, R. M., Jr., and Matson, S. W. (1996) *J. Biol. Chem.* **271,** 25360–25368
28. Subramanya, H. S., Bird, L. E., Brannigan, J. A., and Wigley, D. B. (1996) *Nature* **384,** 379–383
29. Husain, I., Van-Houten, B., Thomas, D. C., Abdel-Monem, M., and Sancar, A. (1985) *Proc. Natl. Acad. Sci. U. S. A.* **82,** 6774–6778
30. Caron, P. R., Kushner, S. R., and Grossman, L. (1985) *Proc. Natl. Acad. Sci. U. S. A.* **82,** 4925–4929
31. Lahue, R. S., Au, K. G., and Modrich, P. (1989) *Science* **245,** 160–164
32. Horii, Z. I., and Clark, A. J. (1973) *J. Mol. Biol.* **80,** 327–344
33. Mendonca, V. M., Kaiser-Rogers, K., and Matson, S. W. (1993) *J. Bacteriol.* **175,** 4641–4651
34. Mendonca, V. M., Klepin, H. D., and Matson, S. W. (1995) *J. Bacteriol.* **177,** 1326–1335
35. Schellhorn, H. E., and Low, K. B. (1991) *J. Bacteriol.* **173,** 6192–6198
36. Arthur, H. M., and Lloyd, R. G. (1980) *Mol. & Gen. Genet.* **180,** 185–191
37. Feinstein, S. I., and Low, K. B. (1986) *Genetics* **113,** 13–33
38. Morel, P., Hejna, J. A., Ehrlich, S. D., and Cassuto, E. (1993) *Nucleic Acids Res.* **21,** 3205–3209
39. Washburn, B. K., and Kushner, S. R. (1991) *J. Bacteriol.* **173,** 2569–2575
40. Taucher-Scholz, G., and Hoffman-Berling, H. (1983) *Eur. J. Biochem.* **137,** 573–580
41. Matson, S. W. (1986) *J. Biol. Chem.* **261,** 10169–10175
42. Runyon, G. T., and Lohman, T. M. (1989) *J. Biol. Chem.* **264,** 17502–17512
43. Runyon, G. T., Bear, D. G., and Lohman, T. M. (1990) *Proc. Natl. Acad. Sci. U. S. A.* **87,** 6383–6387
44. Brosh, R. M., Jr., and Matson, S. W. (1997) *J. Biol. Chem.* **272,** 572–579
45. Zhu, L., and Weller, S. K. (1992) *J. Virol.* **66,** 469–479
46. Martinez, R., Shao, L., and Weller, S. K. (1992) *J. Virol.* **66,** 6735–6746
47. Ma, L., Westbroek, A., Jochemsen, A. G., Weeda, G., Bosch, A., Bootsma, D., Hoeijmakers, J. H. J., and van der Eb, A. J. (1994) *Mol. Cell. Biol.* **14,** 4126–4134
48. Lechner, R. L., and Richardson, C. C. (1983) *J. Biol. Chem.* **258,** 11185–11196
49. Runyon, G. T., Wong, I., and Lohman, T. M. (1993) *Biochemistry* **32,** 602–612
50. Kunkel, T. A., Bebenek, K., and McClary, J. (1991) *Methods Enzymol.* **204,** 125–139
51. Chao, K., and Lohman, T. M. (1990) *J. Biol. Chem.* **265,** 1067–1076
52. Matson, S. W., and Richardson, C. C. (1985) *J. Biol. Chem.* **260,** 2281–2287
53. Yong, Y., and Romano, L. J. (1995) *J. Biol. Chem.* **270,** 24509–24517
54. Matson, S. W., and Richardson, C. C. (1983) *J. Biol. Chem.* **258,** 14009–14016
55. Nevers, P., and Spatz, H. (1975) *Mol. & Gen. Genet.* **139,** 133–143
56. Glickman, B. W., and Radman, M. (1980) *Proc. Natl. Acad. Sci. U. S. A.* **77,** 1063–1067
57. Kuemmerle, N. B., and Masker, W. E. (1980) *J. Bacteriol.* **142,** 535–546
58. Fersht, A. (1985) *Enzyme Structure and Mechanism,* 2nd Ed., pp. 98–120, W. H. Freeman and Co., New York
59. Kornberg, A., and Baker, T. A. (1992) *DNA Replication,* 2nd Ed., W. H. Freeman and Co., New York
60. Matson, S. W., and George, J. W. (1987) *J. Biol. Chem.* **262,** 2066–2076